

Modeling the Effect of Water Diversion on the Temperature of Mountain Streams

Werner Meier¹; Cyrill Bonjour²; Alfred Wüest³; and Peter Reichert⁴

Abstract: Water diversion for hydroelectric power generation impacts the temperature of mountain streams. Such changes are estimated by using a coupled one-dimensional dead-zone heat balance model. In very steep river sections, the dissipation of kinetic energy is the dominant heat source. For such streams, water diversion has only a minor effect on water temperature, because dissipation-induced temperature changes are independent of discharge. In contrast, in river sections of gradual slope, the influence by solar radiation, long-wave radiation, and heat exchange with the streambed is stronger. In such cases, a discharge reduction can lead to significant temperature changes. For a small stream in the southern Swiss Alps, model results show that diversion increases temperature by about 3.7 (± 0.9)°C in a 21 km long river section under high solar radiation during summer. During a cold winter episode, water temperature is estimated to be about 1.8 (± 0.8)°C lower compared to natural conditions. This heat balance model can also be used to simulate the effect of different measures to reduce water temperature changes in affected streams.

DOI: 10.1061/(ASCE)0733-9372(2003)129:8(755)

CE Database subject headings: Mountain streams; Water temperature; Heat balance; Hydroelectric power.

Introduction

Water temperature is an important ecological parameter in mountain streams (Ward 1992) and should be considered in water diversion assessments. It not only affects physical and chemical processes but also the composition and activity of river-borne biotic communities. Due to the smaller depth, and in some cases also due to the longer residence time, small mountain streams are much more susceptible to natural energy fluxes than large and deep lowland rivers. The natural heat fluxes influencing water temperature in mountain streams include solar radiation, energy exchange with the atmosphere, heat exchange with the streambed at the sediment-water interface, heat input from tributaries, internal heat sources, and groundwater in- and exfiltration.

In addition to these natural energy sources, numerous anthropogenic disturbances influence stream temperature as well: water diversion, reservoir storage, hydroelectric power generation, the use of cooling water by thermal power plants, deforestation

and—in the future most probable—anthropogenically caused climate change. Seasonal mean temperature and natural daily temperature variations in the stream can be artificially changed by these disturbances.

Hydroelectric power plants have direct and indirect influence on water temperature. While the potential energy of diverted water is transformed into electricity, friction is transforming this energy into heat in nondiverted waters. As a result, the water in power plant outlets is colder than the water cascading down the river. In addition, low flow rivers have more efficient net heat exchange with the atmosphere and the sediment due to larger surface/volume ratios and longer residence time. As a result, the water temperature along the river increases more during summer and decreases more during winter compared to natural conditions.

The impact of hydropower plants on stream temperature can be estimated by measuring water temperature and energy fluxes under different flow and meteorological conditions. However, it is difficult to collect data under all relevant conditions, because water releases are expensive and meteorological conditions cannot be foreseen. Alternatively, the impact of hydroelectric power plants on stream temperature can be calculated with a heat balance model. It allows predicting water temperature for different stream discharges and meteorological conditions.

In order to overcome the measurement difficulties and to be able to extrapolate water temperatures to situations without observations, a hydraulic and heat balance model was applied to rivers in the Blenio Valley (southern Swiss Alps). The uncertainty in the predictions is considerably reduced by model calibration with data collected in those rivers during a measurement campaign. The heat transport model consists of a dead zone model for substance transport in mountain streams described in Meier (2002) and an attached heat balance model. The heat balance model (Bonjour 1998) builds on previous river temperature modeling efforts (Edinger et al. 1968; Brown 1969; Brown and Barnwell 1987; Sinokrot and Stefan 1993; Webb and Zhang 1997; Evans et al. 1998). A similar model was used to investigate effects of cooling water from a nuclear power plant on the River Aare in

¹PhD, Swiss Federal Institute of Technology Zürich (ETHZ) and SIAM Dept., Swiss Federal Institute for Environmental Science and Technology (EAWAG), Ueberlandstrasse 133, CH-8600 Dübendorf, Switzerland. E-mail: wmeier@eawag.ch

²Environmental Scientist, Bonjour Engineering GmbH, Kirchmattstr. 28, 4654 Lostorf SO, Switzerland. E-mail: cyrill.bonjour@gmx.ch

³Professor, Head of APEC Dept., Swiss Federal Inst. for Environmental Science and Technology (EAWAG), Seestrasse 79, CH-6047 Kastanienbaum, Switzerland. E-mail: wuest@eawag.ch

⁴Professor, Head of SIAM Dept., Swiss Federal Institute for Environmental Science and Technology (EAWAG), Ueberlandstrasse 133, CH-8600 Dübendorf, Switzerland. E-mail: reichert@eawag.ch

Note. Associate Editor: Robert G. Arnold. Discussion open until January 1, 2004. Separate discussions must be submitted for individual papers. To extend the closing date by one month, a written request must be filed with the ASCE Managing Editor. The manuscript for this paper was submitted for review and possible publication on August 6, 2001; approved on July 18, 2002. This paper is part of the *Journal of Environmental Engineering*, Vol. 129, No. 8, August 1, 2003. ©ASCE, ISSN 0733-9372/2003/8-755-764/\$18.00.

Switzerland (Meier 1996). Coupled with the hydraulic and transport model of mountain streams, the heat balance model is used to estimate the effect of various water diversion scenarios in different seasons on the water temperature in selected streams in the Blenio Valley.

Heat Transport Model

Hydraulic Model

For the description of river hydraulics, as well as substance and heat transport, a dead-zone model is used to simulate the effects of pools and lateral storage zones of mountain streams. Water flow in the advective zone of this model is calculated using the diffusive wave approximation to the St. Venant equations for open channel flow (Yen 1973). Darcy-Weisbach friction factors are estimated using the equations proposed by Bathurst (1985). These estimators are adequate for the description of flow in the advective zone because Bathurst carefully avoided the presence of pools in his investigation reaches. In addition to the advective zone, a dead zone is introduced as a simplified representation of pools and lateral storage zones. The hydraulic model and the calibrations of the hydraulics and transport model for the rivers in the Blenio Valley are described in more detail in Meier (2002). In this paper, the calibrated hydraulics and transport model was used as a basis for the heat balance model.

Heat Balance Equations

The hydraulic model described above is appropriate for the description of transport and spreading of tracer pulses in mountain streams. For a temperature model, however, additional storage capacity of heat at a much longer time scale has to be considered (Sinokrot and Stefan 1993). The simplest approach to do this is the introduction of a sediment zone coupled to the water column by heat exchange. This sediment zone summarizes the effect of heat storage by boulders in the riverbed, by sediment material, and by sediment pore water. The empirical heat exchange process between the water column and the sediment zone thus summarizes heat conduction and heat exchange induced by water exchange at a much longer time scale (hours to days) than the exchange with the dead zone (seconds to minutes).

To calculate heat balances for these three zones, three differential equations are required for the temperature changes in the advective zone (1), in the dead zone (2) and in the sediment layer (3), respectively. All equations are formulated for the temporal change of heat per unit river length:

$$\begin{aligned} \rho c_p \frac{\partial (A_{adv} T_{adv})}{\partial t} = & -\rho c_p \frac{\partial (QT_{adv})}{\partial x} + \rho c_p \frac{\partial}{\partial x} \left(A_{adv} E_{adv} \frac{\partial T_{adv}}{\partial x} \right) \\ & + \rho c_p q_{ex} (T_{pool} - T_{adv}) + \gamma w K (T_{sed} - T_{adv}) \\ & + \rho c_p q_{lat} T_{lat} + w H_{adv} \end{aligned} \quad (1)$$

$$\begin{aligned} \rho c_p \frac{\partial (A_{pool} T_{pool})}{\partial t} = & -\rho c_p q_{ex} (T_{pool} - T_{adv}) + (1 - \gamma) w K \\ & \times (T_{sed} - T_{pool}) + w H_{pool} \end{aligned} \quad (2)$$

$$\begin{aligned} \rho c_p^{sed} \frac{\partial (A_{sed} T_{sed})}{\partial t} = & -\gamma w K (T_{sed} - T_{adv}) - (1 - \gamma) w K \\ & \times (T_{sed} - T_{pool}) + w H_{sed} \end{aligned} \quad (3)$$

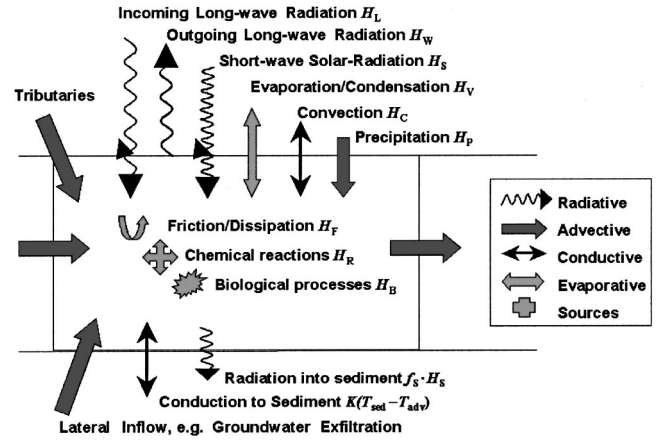


Fig. 1. Scheme of energy fluxes that influence temperature of mountain streams

where $t(s)$ =time; $x(m)$ =distance along the river; $\rho = 1,000 \text{ kg m}^{-3}$ (water density); ρ_{sed} =density of sediment material; $c_p = 4,180 \text{ J kg}^{-1} \text{ K}^{-1}$ (heat capacity of water); c_p^{sed} =heat capacity of sediment material; T_{adv} (K)=temperature in the advective zone; T_{pool} (K)=temperature in the pool zone; T_{lat} (K)=temperature of lateral inflow= T_{in} if $q_{lat} > 0$ (inflow) or T_{adv} if $q_{lat} \leq 0$ (outflow); T_{sed} (K)=temperature in the sediment zone; A_{adv} (m^2)=wetted cross-sectional area of the advective zone; A_{pool} (m^2)=cross-sectional area of the pool zone; A_{sed} (m^2)=cross-sectional area of the sediment zone; Q ($\text{m}^3 \text{ s}^{-1}$)=stream discharge; E_{adv} ($\text{m}^2 \text{ s}^{-1}$)=longitudinal dispersion coefficient in the advective zone; γ (-)=fraction of heat transfer between water column and sediment that leads to exchange with the advective zone ($1 - \gamma$ is the fraction of exchange with the pool zone); K ($\text{W m}^{-2} \text{ K}^{-1}$)=heat transfer coefficient between water column and sediment zone; w (m)=surface width of river; q_{ex} ($\text{m}^3 \text{ s}^{-1} \text{ m}^{-1}$)=exchange coefficient between advective and stagnant water zone; q_{lat} ($\text{m}^3 \text{ s}^{-1} \text{ m}^{-1}$)=lateral inflow (positive) or outflow (negative); H_{adv} (W m^{-2})=input of heat from internal and external sources to the advective zone (Fig. 1); H_{pool} (W m^{-2})=input of heat from internal and external sources to the pool zone (Fig. 1); H_{sed} (W m^{-2})=input of heat from internal and external sources to the sediment zone (Fig. 1). Several unknown parameters in Eq. (3) were combined to form an empirical parameter k [Eq. (4)] for the heat storage capacity of the sediment. This parameter is estimated by comparing simulation results with data.

$$k = \frac{A_{sed} \rho_{sed} c_p^{sed}}{w} \quad (4)$$

The temporal rate of change of heat in the advective zone [Eq. (1), first term] is caused by advection (second term), longitudinal dispersion (third term), exchange with the pool and sediment zones (fourth and fifth terms), lateral in- or outflows (sixth term), and input from internal and external sources (seventh term). Lateral in- or outflows consist of runoff, precipitation, exfiltration from, or infiltration to groundwater or many different small tributaries. Larger tributaries are considered as boundary conditions at node points, where river sections are connected. The extraction of diverted water, the inflow of heated cooling water, and the discharge of water from the power plant must also be considered at node points. Eq. (2) shows that the temporal rate of change of heat in the pool zone (first term) is determined by exchange with

the advective and sediment zones (second and third terms), and by input from internal and external sources (fourth term). The rate of change of heat in the sediment zone [Eq. (3), first term] is determined by exchange with the advective and pool zones (second and third terms), and by input from internal and external sources (fourth term).

The factor γ , which quantifies the distribution of the energy exchanged with the sediment to the advective and the pool zones, depends on the geometry of the river bed and the structure of the flow. A reasonable approximation would be to set this factor equal to the ratio of the advective zone cross section to the total cross-sectional area of the river. However, because the exchange between the advective and the pool zone is much faster (seconds to minutes) than exchange between the water column and the sediment (hours to days), the model results are insensitive to the selection of the value of the factor γ . In our calculations, the factor γ was set to unity.

The heat balance is influenced by energy fluxes through the air-water interface $H_S + H_L + H_W + H_V + H_C$ (solar radiation, incoming long-wave radiation, outgoing long-wave radiation, evaporation or condensation, and convection), and by dissipation of kinetic energy H_F (Fig. 1). Because of fast mixing between advective and pool zones, it is not relevant, for temperature simulations, how the heat exchange with external sources or sinks is distributed between these two zones (this is analogous to the insensitivity of the model to the factor γ explained above). If external heat exchange is attributed to the advective zone, the following expressions result

$$\begin{aligned} H_{\text{adv}} &= (1 - f_s)H_S + H_L + H_W + H_V + H_C + H_F \\ H_{\text{pool}} &= 0 \\ H_{\text{sed}} &= f_s H_S \end{aligned} \quad (5)$$

Here, f_s = fraction of solar radiation entering the water column that reaches the sediment. Throughout the paper, incoming heat fluxes are treated as being positive. The source and sink terms are illustrated in Fig. 1. In the following section these energy fluxes are discussed.

Energy Fluxes through Air-Water Interface

Incoming Short-Wave Radiation

The solar radiation (wave length between 0.14 and 4.0 μm) outside the atmosphere H_S^g is calculated based on the solar constant, the declination angle of the sun, latitude of the site, and the number of hours since midnight (Brock 1981). Clouds and greenhouse gases scatter and absorb a fraction of the solar radiation on its way through the atmosphere. On an overcast day, 65% of the solar radiation is reflected and absorbed by clouds. The calculated solar radiation on the ground H_S^g may be approximated by (Brown and Barnwell 1987)

$$H_S^g = a_i(1 - 0.65C^2)H_S^0 \quad (6)$$

where $a_i(-)$ = atmospheric transmissivity; and $C(-)$ = fraction of cloud cover.

The atmospheric transmissivity can be assumed to be equal to 1 (McCutcheon 1989). The fraction of cloud cover is only measured at a few meteorological stations. There is another possibility to determine the fraction of cloud cover $C(-)$; estimation by a comparison of calculated and measured solar radiation near the ground, and application of Eq. (6). Note that the latter technique cannot be applied during nighttime.

Table 1. Proposed Values for Empirical Constants a and b in Reflectivity Eq. (8)

Clouding (C)	Cloudless (0)	Scattered (0.1–0.5)	Broken (0.6–0.9)	Overcast (1.0)
a	1.18	2.19	0.96	0.36
b	-0.77	-0.97	-0.68	-0.44

The easiest way to determine the net solar radiation entering the water column H_S is to measure the solar radiation H_S^g on the ground near the stream. The measured values of H_S^g can then be converted to values of H_S by considering the reflectivity of the water surface and the shading of the stream by bank vegetation

$$H_S = (1 - k_s)(1 - r_s)H_S^g \quad (7)$$

where $k_s(-)$ = fraction of solar radiation that is blocked by shading of the water surface by steep stream-banks, stream-bank vegetation, or precipitous topography; $r_s(-)$ = total reflectivity of the water surface for short-wave radiation with maximum values of 1; and H_S^g (W m^{-2}) = measured solar radiation near the stream.

Values for k_s are difficult to estimate because of the complicated geometry of the skyline, varying stream bank vegetation, and changing direction of the stream. Therefore, values of k_s may depend on season and time of day.

The reflectivity r_s can be estimated with the equation of Anderson (1954)

$$r_s = a\varphi^b \quad (8)$$

where φ (degrees) = solar angle; and $a(-)$ and $b(-)$ = empirical constants.

Anderson (1954) distinguished values for the parameters a and b for low and high clouds, but in fact the height of clouds is difficult to determine. Therefore, mean values (Table 1) were computed for the different cloud fractions (Brown and Barnwell 1987). For overcast situations with values of C near 1.0, a and b are strongly dependent on the height of clouds. Mean values of a and b for C close to 1 are therefore uncertain.

Incoming Long-Wave Radiation

Incoming long-wave radiation is the radiation from the atmosphere with wavelength between 4 and 120 μm with a maximum at 10 μm wavelength (infrared). This radiation is determined by the Stefan-Boltzmann equation combined with factors for the atmospheric emissivity and the reflectivity of the water surface

$$H_L = (1 - r_L)E_A\sigma T_A^4 \quad (9)$$

where $r_L(-)$ = total reflectivity of the water surface for long-wave radiation; $\sigma = 5.67 \cdot 10^{-8} \text{ W m}^{-2} \text{ K}^{-4}$ (Stefan-Boltzmann constant); $E_A(-)$ = long-wave emissivity of the atmosphere; and T_A (K) = absolute temperature of the atmosphere.

Total reflectivity for long-wave radiation r_L was previously determined to be approximately 0.030 for a source temperature between 0 and 30°C (Anderson 1954).

For the emissivity of the atmosphere, many equations have been proposed (Livingstone and Imboden 1989). These equations take into account atmospheric temperature, cloud cover, cloud height, moisture, and atmospheric constituents like ozone or carbon dioxide. A practicable and fairly accurate equation is the combination of Brutsaert's (1982) equation with Bolz's (1949) equation for consideration of cloudiness

$$E_A = (1 + cC^2)1.24 \left(\frac{e_A}{T_A} \right)^{1/7} \quad (10)$$

where e_A (mbar)=vapor pressure in the atmosphere. For the value of c , Brutsaert (1982) lists a range from 0.04 for Cirrus to 0.25 for Nimbostratus with an average of 0.22.

If it is possible to measure the incoming long-wave radiation near the stream H_L^g (W m^{-2}), Eq. (9) reduces then to

$$H_L = (1 - r_L)H_L^g \quad (11)$$

Outgoing Long-Wave Radiation

The water surface radiates energy almost like a black body. Therefore, a Stefan-Boltzmann equation, extended by the emissivity factor for the water surface of $E_W = 0.970 \pm 0.005$ (Anderson 1954), is considered appropriate.

$$H_W = -E_W \sigma T_W^4 \quad (12)$$

Evaporation/Condensation

If water evaporates from the stream, it loses the latent heat of vaporization and the sensible heat of the evaporated water. Rarely the air temperature falls below the dew-point, and condensation takes place.

$$H_V = -\rho M_{\text{eva}} [L_V + c_p(T_E - T_W)] \quad (13)$$

where $L_V = 2.450 \cdot 10^6 \text{ J kg}^{-1}$ (latent heat of water vaporisation); T_E (K)=temperature of the evaporated water; and M_{eva} (ms^{-1}) = evaporation rate (mostly given in millimeter per day). The second term is assumed to be negligible because L_V is much larger than $c_p(T_E - T_W)$. The evaporation rate can be estimated as

$$M_{\text{eva}} = f_M^0 \nu_{\text{eva}} \frac{e_w - e_A}{p/1,000} \quad (14)$$

where f_M^0 (-)=dimensionless wind function for evaporation; ν_{eva} (ms^{-1})=exchange velocity for latent heat of vaporization; p (mbar)=air pressure; e_w (mbar)=vapor pressure at temperature of surface water; and e_A (mbar)=vapor pressure of the atmosphere.

All constant parameters in Eqs. (13) and (14) are summarized in an extended wind function f_M , which yields the simplified equation

$$H_V = -f_M(e_w - e_A) \quad (15)$$

The new wind function f_M ($\text{W m}^{-2} \text{ mbar}^{-1}$) depends also on the wind velocity over the water surface and on the stratification of the lower part of the atmosphere above the stream, which can be expressed using the difference between the water and air temperature (Livingstone and Imboden 1989).

$$f_M = p_1 + p_2 u_{10} + p_3 (T_W - T_A) \quad (16)$$

where u_{10} (ms^{-1})=wind velocity measured at 10 m height above the stream and p_1 ($\text{W m}^{-2} \text{ mbar}^{-1}$); p_2 ($\text{W m}^{-2} \text{ mbar}^{-1} \text{ m}^{-1} \text{ s}$); and p_3 ($\text{W m}^{-2} \text{ mbar}^{-1} \text{ K}^{-1}$)=empirical factors.

These factors cannot be measured directly and must be estimated by a comparison of model results with data. The parameter estimation should be restricted to river sections with small solar radiation due to shading and with a small heat exchange rate with the sediment in order to become sensitive to these fluxes. The following values, which were estimated for a similar stream (but with smaller slope) in Switzerland (Meier 1996), were used:

$$p_1 = 13 \text{ W m}^{-2} \text{ mbar}^{-1}, \quad p_2 = 0.86 \text{ W}^{-2} \text{ mbar}^{-1} \text{ m}^{-1} \text{ s}$$

and

$$p_3 = 0.17 \text{ W m}^{-2} \text{ mbar}^{-1} \text{ K}^{-1}$$

Convection

Convection is the transfer of sensible heat through the air-water interface. The convective heat flux can be estimated as

$$H_C = f_M^* \rho c_p \nu_{\text{cond}} (T_W - T_A) \quad (17)$$

where ν_{cond} (ms^{-1})=exchange velocity for convection at the air-water interface; and f_M^* =dimensionless wind function for convection.

The Bowen ratio (Bowen 1926) of heat loss by convection to that by evaporation is

$$\frac{H_C}{H_V} = B \frac{T_W - T_A}{e_w - e_A} p/1,000 \quad (18)$$

$$B = \frac{f_M^* c_p \nu_{\text{cond}}}{f_M^0 L_V \nu_{\text{eva}}} \quad (19)$$

The value for the Bowen factor B was estimated by Bowen (1926) to be about 0.61 K^{-1} . Other estimates for B range between 0.57 K^{-1} for smooth and 0.66 K^{-1} for rough water surface (unpublished values of Pritchard in Anderson 1954). For mountain streams with their usually rough surface, a value of 0.66 K^{-1} for B was chosen. The heat loss by convection can be expressed with the Bowen factor, the wind function f_M , air pressure, and the temperature difference.

$$H_C = -B f_M (T_W - T_A) p/1,000 \quad (20)$$

Precipitation

Webb and Zhang (1997) and Evans et al. (1998) measured the volume and temperature of incoming rainfall and judged the energy flux due to precipitation to be insignificant, even on days with heavy rainfalls. However, snowfall may influence the heat budget, since the latent heat of melting is high ($L_M = 3.34 \times 10^5 \text{ J kg}^{-1}$ at 20°C).

Internal Heat Sources

Dissipation

In river sections with gradual slopes, viscous dissipation of turbulent kinetic energy results in a negligible contribution to other heat sources. However, in very steep mountain streams, this flux can be even dominant. Almost the entire potential energy is dissipated into heat. Negligible amounts go into sound and transport and destruction of bed material. Expressed as a heat flux per unit of the surface area of the river (Evans et al. 1998), dissipation can be expressed as

$$H_F = \rho g S_0 \frac{Q}{w} \quad (21)$$

where g (ms^{-2})=gravitational acceleration; and S_0 (-)=slope of river bed.

Temperature increase by dissipation can easily be calculated by converting potential energy ($mg\Delta h$) to heat ($mc_p\Delta T$)

$$\frac{\Delta T}{\Delta h} = \frac{g}{c_p} = \frac{0.235^\circ\text{C}}{100 \text{ m}} \quad (22)$$

where Δh (m)=difference in elevation; and ΔT (K)=temperature increase.

Chemical and Biological Processes

Heating due to chemical or biological degradation is negligible in nonpolluted streams (Anderson 1954; Evans et al. 1998).

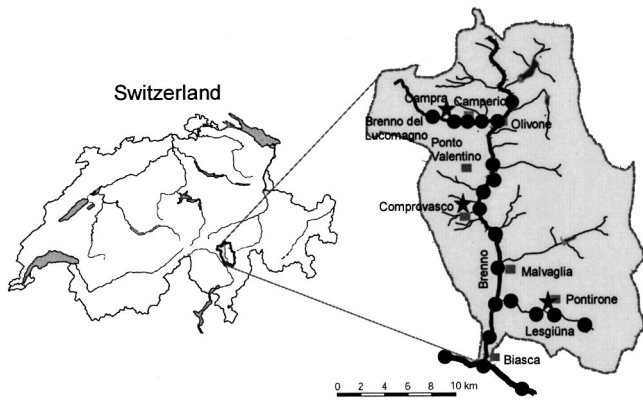


Fig. 2. Map of Blenio valley with temperature measurement sites (dots) and location of meteorological stations (stars)

Study Sites and Measurement Techniques

Study Site

The field study took place in the Valley Blenio in the southern Swiss Alps. The main valley, formed by a glacier, is oriented from north to south. The catchment area covers 397 km² with an average altitude of 1,820 m above sea level. The River Brenno has a mean slope of about 3%, and the tributaries are even steeper with slopes up to 15%. Mean width of the river varies from 6 to 15 m and mean depth from 0.1 to 0.3 m. The annual flow regime at the lower end of the catchment area near Biasca (Fig. 2) shows a seasonal minimum flow in winter and a maximum flow in summer with a mean flow of about 4.7 m³ s⁻¹. Without water diversion, discharge would be about three times larger.

Water Temperature

Water temperature was measured at 35 locations in the River Brenno and in two of its tributaries, Lesgiuna and Brenno del Lucomagno (Fig. 2). Values were recorded at 10 min intervals using two types of miniature self-contained temperature data-loggers (Vemco, Shad Bay, Canada) with an accuracy of 0.1 and 0.2°C, respectively. At some locations the temperature of the sediment was measured with data-loggers which were buried manually or accidentally during flood events.

Meteorological Parameters

A station of the Swiss Meteorological Institute (<http://www.meteoschweiz.ch/en/>) measures meteorological parameters in the main valley at 300 m distance from the stream (Fig. 2). The air temperature and relative humidity instruments are housed in standard enclosures at standard heights. In two side valleys, an Aanderaa (Bergen, Norway) meteorological station was installed within 100 m distance of the stream (Fig. 2). The following meteorological parameters were measured in 10 min intervals (accuracy in parentheses): short-wave radiation (20 W m⁻²), long-wave radiation (3%), air temperature (0.1°C), wind velocity (2%), wind direction (5°), relative humidity (3%), precipitation (unknown), and air pressure (0.2 mbar).

Hydraulic Parameters

The hydraulic parameters discharge, mean velocity, and longitudinal dispersion were measured with tracer experiments using

chloride and uranine injections. At the lower end of the catchment area, in the middle reach of the River Brenno, and before the junction of tributary Lesgiuna, discharge is measured continually by the Swiss Hydrological and Geological Survey (<http://www.bwg.admin.ch/e/>) with an accuracy of 10%.

Stream Morphology

The elevations of the streambeds were extracted from Swiss Topographical Service maps with a scale of 1:25'000 and contour lines with elevation difference of 20 m. Mean width and depth were measured in typical river sections.

Data Analysis Techniques

Heat Balance Model

The definition of the dead-zone model used to describe hydraulics and substance transport, as well as the calibration of this model to the streams in Val Blenio, are described in Meier (2002). In this paper, the hydraulic model is complemented with a heat balance model described by Eqs. (1)–(3) in which the following expressions were used for the source terms given in Eq. (5):

1. Solar radiation: Eq. (7);
2. Incoming long-wave radiation: Eq. (9) with E_A according to Eq. (10) and C from a comparison of measured and calculated solar radiation (Brock 1981) and by solving Eq. (6) for C ;
3. Outgoing long-wave radiation: Eq. (12);
4. Evaporation/Condensation: Eq. (15) with the wind function given by Eq. (16);
5. Convection: Eq. (20); and
6. Dissipation: Eq. (21).

There was no rain or snow-fall during the simulated periods so the energy flux precipitation could be omitted. Possible effects of groundwater exfiltration on water temperature, which could not be measured, were neglected.

Parameter Estimation

The parameters of the hydraulics and substance transport model were estimated using tracer tests [see Meier (2002) for details]. The empirical coefficients of the wind function were estimated for another river, where evaporation was more important to the total heat flux. The uncertainty resulting from the use of these coefficients for the streams in the Blenio Valley is small because evaporation, condensation, and convection are only small fractions of the total heat flux in this application. The shaded fraction of the stream surface k_s , the fraction of short-wave radiation entering the sediment f_s , the heat storage capacity of the sediment k [according to Eq. (4)], the heat exchange coefficient of the sediment K , and the initial value of sediment temperature $T_{sed,ini}$, were estimated by weighted least-squares parameter estimation. The last parameter could be eliminated from the fit by starting the simulation several days before the start of the temperature time series used for the fit. The estimation for the fraction of short-wave radiation entering the sediment was always zero.

Validation

The model was validated in two ways. First, calculated and measured time series were compared. Second, mean values of a

longer period in early summer were checked with cross validation (Power 1992). The model, which was calibrated with a time series of five days (6/17/98 to 6/22/98), was applied to a time period of eight weeks (5/1/98 to 6/26/98). The calculated daily mean values were compared with measured ones. The resulting r^2 for the correlation is 0.96 for daily mean temperature. The corresponding value for daily maximum and minimum temperature is 0.90 and 0.92, respectively.

Uncertainty Analysis

The uncertainty of model results was estimated with linear error propagation techniques. The estimates of parameter uncertainty and numerically approximated partial derivatives of stream temperature with respect to model parameters were used to estimate the standard deviation of calculated temperature according to

$$\sigma_{T_{adv}} = \sqrt{\sum_{i=1}^m \left(\frac{\partial T_{adv}}{\partial p_i} \right)^2 \sigma_{p_i}^2} \quad (23)$$

where $\sigma_{T_{adv}}$ = approximate standard deviation of the model result; p_i = model parameter i ; and σ_{p_i} = standard deviation (uncertainty) of parameter i . Correlation between the parameters is neglected.

Scenarios

Mountain streams typically have steep slopes. The steeper the slope of a river section, the higher is the impact of dissipation on water temperature. Therefore, two short sections with different slopes, one in the tributary Brenno del Lucomagno near Camperio (slope of 14.4%) and one in the main section of River Brenno near Ponto Valentino (slope of 3.8%) were compared (Fig. 2). A hypothetical decrease in discharge of 50% was assumed in order to quantify the impact of water diversion on water temperature in these two sections.

Two situations in summer and two in winter with and without water diversion were calculated in the 20.6 km long main section of River Brenno between Olivone and Biasca in order to infer the thermal effect of diversion. In this reach with a gradual slope and a wide river bed, the largest impact of water diversion is expected.

Numerical Simulations

All numerical simulations, parameter estimations and sensitivity analyses were done using *AQUASIM*, a computer program for simulation and data analysis of aquatic systems [Reichert (1994) or (<http://www.aquasim.eawag.ch>)]. Thirty minutes were chosen as an output time interval. The along-river grid resolution was set to 20 m.

Results

Comparison of Steep and Gently Sloped River Sections

A steep section in the tributary Brenno del Lucomagno was compared to a gently sloped section in the River Brenno. For this comparison, a period of two days in summer 1998 with high solar radiation was chosen. The steep section has a mean slope of 14.4% and a length of 2.5 km. Due to the small mean width of 6

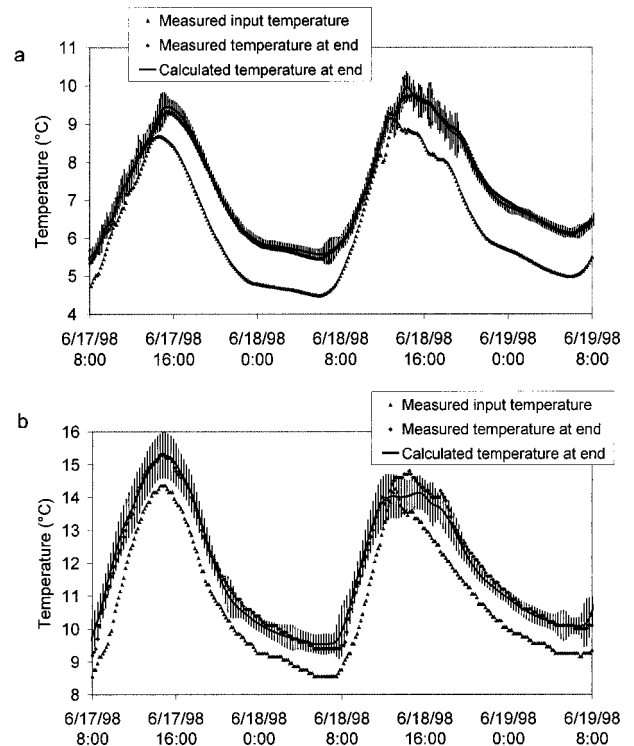


Fig. 3. Measured and calculated water temperature (with uncertainty) at beginning and end of steep river section (14.4%) of Brenno del Lucomagno near Camperio (a) and of gently sloped river section (3.8%) of Brenno near Ponto Valentino (b), respectively.

to 12 m and the riparian forest, this section is strongly shaded. With visual estimation the shading fraction was set to 70%. The gently sloped section has a slope of 3.8% and is 3.9 km long. Here, the broad stream flows through flood plains in a north-south direction and is only weakly shaded. The shading fraction was visually estimated to be about 14% for this stream section. The parameter estimation algorithm led in both cases to estimates of zero for the fraction of short-wave radiation heating the sediment.

Measured and calculated water temperatures show excellent agreement (Fig. 3). The water temperature increases in both sections by about 1°C due to natural energy fluxes. For these two river sections water diversion scenarios with 50% decrease in the actual discharge were computed. Natural discharge of Brenno del Lucomagno (steep) is $2.5 \text{ m}^3 \text{ s}^{-1}$ and for Brenno (gently sloped) a discharge of $1.5 \text{ m}^3 \text{ s}^{-1}$ was measured. The water temperature of the steep section shows almost no temperature change due to water diversion, whereas the water temperature of the gently sloped section is increased by about 0.3°C on average in addition to the natural increase without water diversion.

The reason for the different behavior can be explained with the significance of the contributions of different heat fluxes to the total heat flux. As it is clearly shown in Table 2, the energy flux to the steep river section is dominated by dissipation. Because the effect of dissipation on stream temperature is independent of discharge [see Eq. (22)], only the smaller contributions to the heat flux can have a discharge-dependent effect. The situation is different for the gently sloped stream section. Here, incoming and outgoing long-wave radiation and solar radiation are the dominant heat fluxes. Since the effect of these heat fluxes on temperature is

Table 2. Mean Energy Fluxes in Steep and Gently Sloped River Section

Comparison of a steep (slope=14.4%) and a gently sloped (slope=3.8%) stream sections	(Brenno del Lucomagno)	(Brenno)
	Mean energy flux (W m^{-2})	
Dissipation	1,812	44
Outgoing long-wave radiation	-340	-359
Incoming long-wave radiation	290	293
Solar radiation	110	227
Heat exchange with sediment	-63	-24
Evaporation	-50	-57
Convection	53	38

dependent on the surface to volume ratio of the water body, a more significant effect results from a change in stream discharge.

Simulation of Main Stream from Olivone to Biasca

From this result and the fact that all tributaries of the River Brenno are very steep, we assumed that water diversion has only a small impact on water temperature in the tributaries to the River Brenno. The investigation concentrates on the 20.6 km long gently sloped main section of the River Brenno between Olivone and Biasca (Fig. 2) with an average slope of 2.8%.

Summer Situation

The agreement between calculated and measured temperatures for the actual situation with water diversion is excellent (Fig. 4, top). Only on two cloudy days, 6/18/98 and 6/19/98, the modeled temperatures are slightly too low at noon. The most probable reasons for these deviations are local clouds over the meteorological station or a poor parameterisation of the emissivity of the atmosphere. The most important heat fluxes for this simulation are shown in Fig. 5. During the time period shown in Fig. 5, there is a trend in the direction of heat exchange between the water column to the sediment zone. This is in response to the increase in mean river water temperature. A second simulation for a hypothetical situation without water diversion led to a downstream temperature between 3.7 and 1.4°C lower than that calculated for the actual situation. This implies that the reduction in discharge from 15.5 to 4.9 $\text{m}^3 \text{s}^{-1}$ causes a downstream temperature increase of up to 3.7°C.

Winter Situation

For the winter situation, new values for the shading factor, heat capacity coefficient, and transfer coefficient of the sediment had to be estimated. These properties of the sediment can change during and after a flood event due to flushing and colmatation. All other estimated parameters were taken from the summer situation. In the winter situation, the agreement between calculated and measured temperatures for the actual situation with water diversion is good (Fig. 4, bottom). The temperature estimates for the hypothetical situation without water diversion are by up to 1.8°C higher than measured. Therefore, the reduction in stream discharge from 7.6 to 2.1 $\text{m}^3 \text{s}^{-1}$ caused a reduction in temperature of up to 1.8°C. Again, there is a trend in the heat flux, in this case from the sediment to the water column (Fig. 5).

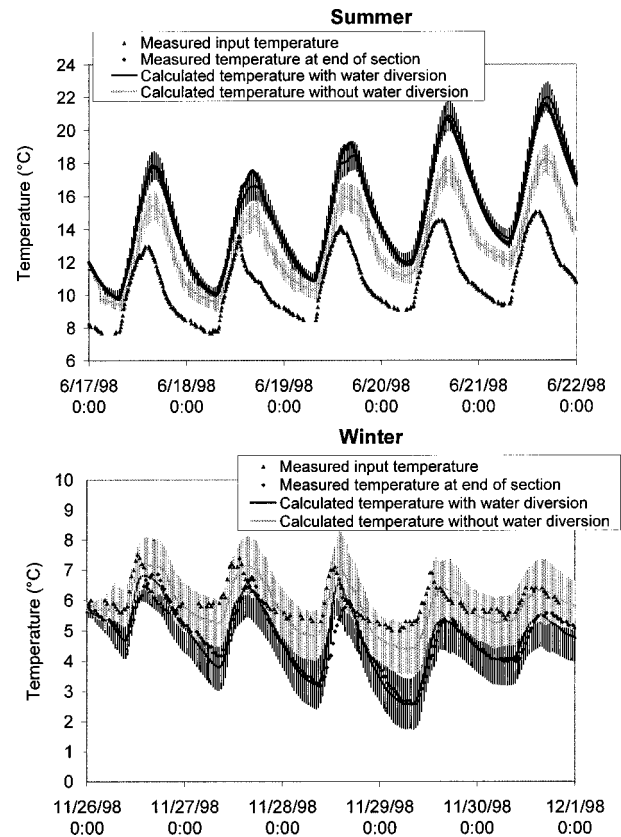


Fig. 4. Measured temperatures (dots) at beginning and end of 20.6 km long main section of River Brenno and modeled temperatures (lines) with uncertainty at end of stretch for actual situation with diversion and hypothetical situation without diversion during five days in summer and winter

Discussion

Comparison with Literature

Table 3 shows a comparison of energy fluxes of the River Brenno with those of three other small streams, where data was available. With the exception of the heat flux resulting from dissipation, which is significantly larger for the steep River Brenno, the energy fluxes are of the same order of magnitude.

Dominant Energy Fluxes

The following factors determine which energy fluxes are dominant in mountain streams: season, slope of the streambed, shading fraction, cloud fraction, and depth of the stream. In streams steeper than 5 to 10%, dissipation is the dominant heat source. At these slopes, dissipation energy input per unit area [Eq. (21)] is of the same order as the maximum summer solar radiation at noon (in latitudes typical for Central Europe about 1,000 W m^{-2}). If the stream is shaded or solar radiation is small, dissipation may dominate also for gradual slopes. Dissipation leads to a temperature increase of 0.24°C per 100 m vertical elevation difference.

Streams with slopes smaller than about 3% and no shading are mainly heated by solar radiation during day and clear sky conditions (Fig. 5). Heat exchange with the sediment can have a significant influence on water temperature as well, at least in the short run.

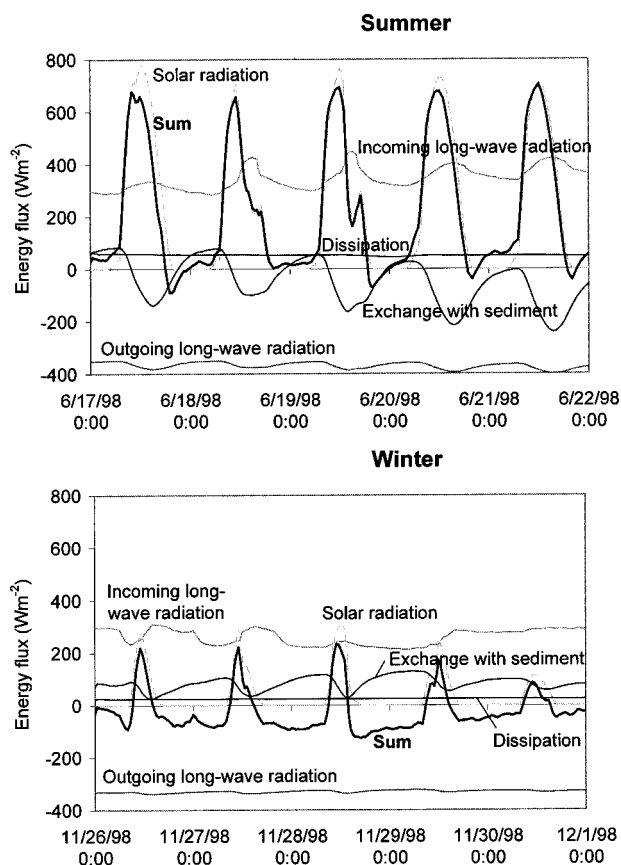


Fig. 5. Calculated energy fluxes for River Brenno in summer and winter (uncertainties, evaporation, and convection are omitted for clarity of presentation)

Net long-wave radiation, evaporation, and conduction become important in gently sloped streams, if short-wave radiation is small due to shading, overcast sky, or weak winter radiation.

Influence of Water Diversion on Water Temperature

The temperature change due to dissipation depends only on the altitude difference and is independent of discharge. This temperature change is equal to $2.4^{\circ}\text{C km}^{-1}$ according to Eq. (22). Artificial changes of discharge have therefore only a small influence on temperature change due to dissipation. In steep, shaded streams, where dissipation is the dominant energy flux, there is almost no temperature change due to water diversion.

If solar radiation and energy exchange with the atmosphere is dominant, there will be an influence of the artificially changed

discharge on water temperature. Water diversion increases the surface to volume ratio of the water body by decreasing water depth. This increases the relative effect of energy exchange on water temperature.

In our example for the River Brenno, the model results show that water temperature may be increased by up to 3.7°C in summer as a result of water diversion. In Switzerland there is a regulation, which requires that the water temperature increase below a cooling water discharge site must not exceed the limit of 3°C . However, this regulations does not apply to water diversion sites. During winter conditions, water diversion in the River Brenno may result in a decrease in water temperature by up to 1.8°C .

Artificially increased water temperatures may have an influence on ecosystems (Ward 1992). If water temperature is altered too much, an increase in discharge, i.e., less water diversion, may improve the situation at least during summer as shown in the river section with gradual slope. Another option may be the plantation of trees along stream benches. Changing the streambed morphology in order to get a smaller water surface would be another option, however, this is usually accompanied by negative impacts on ecosystems.

Conclusions

An extended one-dimensional model describing the river by an advective zone, a stagnant pool zone, and a sediment zone was coupled with a heat balance model. After calibration of a few parameters, this model is able to accurately predict water temperature of the investigated mountain streams for different water diversion scenarios.

The energy fluxes, which significantly influence water temperature of small mountain streams, are solar radiation, long-wave radiation, dissipation of kinetic energy, heat exchange with the sediment, convection, and evaporation. Heat fluxes from groundwater exfiltration, precipitation, and chemical or biological processes may locally play a role, but are usually negligible.

In steep and shaded river sections, dissipation is the dominant energy flux. The temperature increase due to dissipation is independent of discharge and 0.24°C per 100 m elevation drop. Water diversion has therefore little impact on water temperature in such streams.

In river sections of gradual slope solar radiation, heat exchange with the sediment and long-wave radiation are the dominant heat fluxes. In diverted river sections, water temperature along the river is usually increased during the summer, and decreased during the winter, respectively, due to water diversion.

For the River Brenno in the southern Swiss Alps, model results indicate that at the end of a 21 km long river reach the water temperature is increased by about $3.7 (\pm 0.9)^{\circ}\text{C}$ due to water di-

Table 3. Comparison of Calculated Energy Fluxes in Summer for Four Streams

Energy fluxes W m^{-2}	This paper Brenno, CH	Evans et al. (1998) Blithe, UK	Webb and Zhang (1997) Culm 2, UK	Sinokrot and Stefan (1993) Clearwater, USA
Stream	7/21/1998	7/22/1994	8/9/1992–8/17/1992	10/7/1990–10/17/1990
Date				
Short-wave radiation	221	252	77 (All-wave radiation)	76
Long-wave radiation	-25	-109		-63
Heat exchange with sediment	-48	-49	-11	12
Evaporation	-37	-75	-10	-18
Convection	48	2	10	-5
Dissipation	52	1	2	—
Sum	211	22	68	2

version during a summer period of high solar radiation. In a winter situation calculations indicate a decrease in water temperature of about 1.8 (± 0.8)°C due to water diversion. If the water temperature is near 0°C, the additional cooling effect caused by water diversion could lead to build up of ground ice, which may harm fish eggs.

Acknowledgments

The writers thank Michael Schurter for his valuable help during the measurements and Matt Hare for carefully checking the manuscript. The power plant authorities of OFIBLE, the Swiss Meteorological Institute “MeteoSwiss” and the Swiss Federal Office for Water and Geology (BWG) provided essential data for the investigation.

Notation

The following symbols are used in this paper:

- A = cross sectional area [estimated] (m^2);
- a = empirical constant for calculation of r_s (-);
- a_t = atmospheric transmissivity (-);
- B = Bowen factor (K^{-1});
- b = empirical constant for calculation of r_s (-);
- C = fraction of cloud cover (-);
- c = cloud type factor (-);
- c_p = heat capacity of water ($\text{J kg}^{-1} \text{K}^{-1}$);
- c_p^{sed} = heat capacity of sediment material ($\text{J kg}^{-1} \text{K}^{-1}$);
- E_A = long-wave emissivity of atmosphere (-);
- E_{adv} = coefficient of longitudinal dispersion ($\text{m}^2 \text{s}^{-1}$);
- E_W = long-wave emissivity of water surface (-);
- e_A = vapor pressure of atmosphere [measured] (mbar);
- e_S^0 = saturation vapor pressure at reference temperature T_0 (mbar);
- e_w = vapor pressure at temperature of surface water (mbar);
- f_M = wind function ($\text{W m}^{-2} \text{mbar}^{-1}$);
- f_M^0 = dimensionless wind function for evaporation (-);
- f_M^* = dimensionless wind function for convection (-);
- f_s = fraction of short-wave radiation that reaches sediment [estimated from T data] (-);
- g = gravitational acceleration (ms^{-2});
- H = sources and sinks of heat (W m^{-2});
- H_B = energy gain by biological processes (W m^{-2});
- H_C = energy gain by convection (W m^{-2});
- H_F = energy gain by viscous dissipation (W m^{-2});
- H_L = incoming long-wave radiation (W m^{-2});
- H_L^g = incoming long-wave radiation on ground (W m^{-2});
- H_P = energy gain by precipitation (W m^{-2});
- H_R = energy gain by chemical reactions (W m^{-2});
- H_S = solar radiation (W m^{-2});
- H_S^g = solar radiation on ground [measured] (W m^{-2});
- H_S^0 = solar radiation outside atmosphere (W m^{-2});
- H_V = energy loss due to evaporation (W m^{-2});
- H_W = outgoing long-wave radiation (W m^{-2});
- K = heat transfer coefficient of sediment layer [estimated from T data] ($\text{W K}^{-1} \text{m}^{-2}$);

- k = product of ρ_{sed} , c_p^{sed} , and d_{sed} [estimated from T data] ($\text{J K}^{-1} \text{m}^{-2}$);
- k_s = fraction of solar radiation blocked by shading [estimated from T data] (-);
- L_M = latent heat of melting of water (J kg^{-1});
- L_V = latent heat of vaporization of water (J kg^{-1});
- M_{eva} = evaporation rate (mmd^{-1});
- M_W = molecular mass of water (kg mol^{-1});
- p = air pressure [measured] (bar);
- p_i = model parameter i (NA);
- p_1, p_2, p_3 = empirical factors for wind function [estimated] ($\text{W m}^{-2} \text{mbar}^{-1}$, $\text{W m}^{-2} \text{m}^{-1} \text{s mbar}^{-1}$, $\text{W m}^{-2} \text{K}^{-1} \text{mbar}^{-1}$, respectively);
- Q = discharge [measured] ($\text{m}^3 \text{s}^{-1}$);
- q_{ex} = coefficient for exchange between stagnant and advective zone [estimated with tracer experiments] ($\text{m}^2 \text{s}^{-1}$);
- q_{lat} = discharge of lateral inflow per unit length ($\text{m}^2 \text{s}^{-1}$);
- R = universal gas constant ($\text{J K}^{-1} \text{mol}^{-1}$);
- r_L = total water surface reflectivity of long-wave radiation (-);
- r_s = total water surface reflectivity of short-wave radiation (-);
- S_0 = slope of river bed [measured] (-);
- T = temperature (K);
- T_A = air temperature [measured] (K);
- T_E = temperature of evaporated water (K);
- $T_{\text{sed,ini}}$ = initial temperature of sediment layer [estimated from T data] (K);
- T_W = water temperature [input temperature measured] (K);
- t = time (s);
- u_{10} = wind velocity at 10 m height [measured] (ms^{-1});
- w = water surface width of river (m);
- x = distance in flow direction (m);
- γ = fraction of heat transfer between water column and sediment that goes into advective zone (-);
- ΔT = temperature change (K);
- Δh = difference in elevation (m);
- v_{cond} = exchange velocity for convection (ms^{-1});
- v_{eva} = exchange velocity for latent heat of evaporation (ms^{-1});
- ρ = density of water (kg m^{-3});
- ρ_{sed} = density of sediment material (kg m^{-3});
- σ = Stefan-Boltzmann constant ($\text{W K}^{-4} \text{m}^{-2}$);
- σ_{p_i} = standard deviation of parameter i (NA);
- $\sigma_{T_{\text{adv}}}$ = standard deviation of temperature of advective zone (K); and
- φ = solar angle (degrees).

Subscripts and Superscripts

- adv = advective compartment;
- lat = lateral in- or outflow;
- pool = stagnant compartment;
- sed = sediment layer;
- ini = initial; and
- in = input.

References

- Anderson, E. R. (1954). "Energy budget studies, water loss investigations, Lake Hefner studies." *Professional Paper 269*, U.S. Geological Survey, Reston, Va.
- Bathurst, J. C. (1985). "Flow resistance estimation in mountain rivers." *J. Hydraul. Div., Am. Soc. Civ. Eng.*, 111(HY4), 625–643.
- Bolz, H. M. (1949). "Die Abhängigkeit der infraroten Gegenstrahlung von der Bewölkung." *Z. Meteorol.*, 3, 201–203.
- Bonjour, C. (1998). "Modellierung des Wärmeaustausches über die Wasseroberfläche eines Gebirgsbachs." Diploma thesis, EAWAG Dübendorf, Switzerland.
- Bowen, I. S. (1926). "The ratio of heat losses by conduction and by evaporation from any water surface." *Phys. Rev.*, 2(27), 779–787.
- Brock, T. D. (1981). "Calculating solar radiation for ecological studies." *Ecol. Modell.*, 14, 1–19.
- Brown, G. W. (1969). "Predicting temperature of small streams." *Water Resour. Res.*, 5(1), 68–75.
- Brown, L. C., and Barnwell, T. O. (1987). *The enhanced stream water quality models QUAL2E and QUAL2E-UNCAS: Documentation and user manual*, Environmental Research Laboratory, Athens, Greece.
- Brutsaert, W. H. (1982). *Evaporation into the Atmosphere*, Reidel, Dordrecht, The Netherlands.
- Edinger, J. E., Duttweiler, D. W., and Geyer, J. C. (1968). "The response of water temperatures to meteorological conditions." *Water Resour. Res.*, 4(5), 1137–1143.
- Evans, E. C., McGregor, G. R., and Petts, G. E. (1998). "River energy budgets with special reference to river bed processes." *Hydrolog. Process.*, 12, 575–595.
- Livingstone, D. M., and Imboden, D. M. (1989). "Annual heat balance and equilibrium temperature of Lake Aegeri, Switzerland." *Aquatic Sci.*, 51(4), 351–369.
- McCutcheon, S. C. (1989). "Water quality modeling." *Transport and surface exchange in rivers*, Vol. 1, CRC, Boca Raton, Fla.
- Meier, W. K. (2002). "Modellierung der Auswirkungen von Wasserkraftanlagen auf physikalische und chemische Eigenschaften von Bergbächen." Dissertation, ETH, Zürich, Switzerland.
- Meier, W. K. (1996). "Veränderungen des Temperaturhaushaltes der Aare durch das Kernkraftwerk Mühleberg." Diploma thesis, ETH Zürich, Switzerland.
- Power, M. (1992). "The predictive validation of ecological and environmental models." *Ecol. Modell.*, 68, 33–50.
- Reichert, P. (1994). "AQUASIM-A tool for simulation and data analysis of aquatic systems." *Water Sci. Technol.*, 30(2), 21–30.
- Sinokrot, H. G., and Stefan, B. A. (1993). "Stream temperature dynamics: Measurement and modeling." *Water Resour. Res.*, 29(7), 2299–2312.
- Ward, J. V. (1992). *Biology and habitat*, Wiley, New York.
- Webb, B. W., and Zhang, Y. (1997). "Spatial and seasonal variability in the components of the river heat budget." *Hydrolog. Process.*, 11(1), 79–101.
- Yen, B. (1973). "Open-channel flow equations revisited." *J. Eng. Mech. Div., Am. Soc. Civ. Eng.*, 99(5), 979–1009.